

Influences of Temperature, Pressure, and Lattice Solvents on the Spin Transition Regime of the Polymeric Compound $[\text{Fe}(\text{hyetrz})_3]\text{A}_2 \cdot 3\text{H}_2\text{O}$ (hyetrz = 4-(2'-hydroxyethyl)-1,2,4-triazole and $\text{A}^- =$ 3-nitrophenylsulfonate)

Yann Garcia,[†] Petra J. van Koningsbruggen,[†] René Lapouyade,[†]
Léopold Fournès,[†] Louis Rabardel,[†] Olivier Kahn,^{*,†} Vadim Ksenofontov,[§]
Georg Levchenko,[§] and Philipp Gütlich^{*,§}

Laboratoire des Sciences Moléculaires, Institut de Chimie de la Matière Condensée de Bordeaux, UPR CNRS no 9048, 33608 Pessac, France, and Institut für Anorganische und Analytische Chemie, Johannes Gutenberg University, D-55099 Mainz, Germany

Received February 25, 1998. Revised Manuscript Received May 27, 1998

$[\text{Fe}(\text{hyetrz})_3](3\text{-nitrophenylsulfonate})_2 \cdot 3\text{H}_2\text{O}$ (**1**·**3H₂O**), with hyetrz = 4-(2'-hydroxyethyl)-1,2,4-triazole, has been synthesized, and its physical properties have been investigated with several techniques, including optical and Mössbauer spectroscopies, magnetism at different pressures up to ca. 9 kbar, thermogravimetry, calorimetry, and X-ray powder diffraction. At room temperature, **1**·**3H₂O** is in the low-spin (LS) state and the color is pink. As the compound is heated, the three noncoordinated water molecules are released, and the Fe^{2+} sites now undergo a transition from low-spin (LS, $S = 0$) to high-spin (HS, $S = 2$) states. This transformation, denoted as **1**·**3H₂O** (LS) \rightarrow **1** (HS), is irreversible in a normal atmosphere and is accompanied by a change of color between pink and white. Depending on the rate of increasing temperature, it is possible to observe compound **1** in the metastable LS state. The thermal transformation from this metastable state to the stable HS state is then extremely abrupt, occurring within ca. 1 K. Compound **1** has been found to exhibit a spin transition in the low-temperature range, with $T_{1/2}$ around 100 K. This transition is cooperative around $T_{1/2}$, with a thermal hysteresis of about 10 K, but already begins immediately below room temperature. At 4 K, about 15% of the Fe^{2+} sites have been found to remain in the HS state. The pressure dependence of the LS \rightleftharpoons HS transition for **1** has been investigated. A pronounced effect has been observed; the transition temperature is shifted from 100 to 270 K as the pressure varies from 1 bar up to 8.9 kbar.

Introduction

Some $3d^n$ ($4 \leq n \leq 7$) transition metal compounds of octahedral symmetry may exhibit a thermally induced crossover between a low-spin (LS) and a high-spin (HS) state.^{1–8} The fundamental origin of the phenomenon is molecular, but the shape of the temperature dependence of the high-spin molar fraction, $x_{\text{HS}} = f(T)$, depends dramatically upon intermolecular interactions.^{7,9} The more pronounced these intermolecular

interactions are, the steeper the $x_{\text{HS}} = f(T)$ curve around the inversion temperature, $T_{1/2}$, for which there are 50% LS molecules and 50% HS molecules. When the magnitude of these interactions overcomes a threshold value, the spin crossover phenomenon may become cooperative. The thermally induced transitions between LS and HS states may not only be very abrupt but also occur with a hysteresis effect. If it is so, the temperature of the LS \rightarrow HS transition in the warming mode, $T_{1/2}^{\uparrow}$, is higher than the temperature of the HS \rightarrow LS transition in the cooling mode, $T_{1/2}^{\downarrow}$. The existence of hysteresis is of utmost importance, as it confers a memory effect on the system.¹⁰ Between $T_{1/2}^{\uparrow}$ and $T_{1/2}^{\downarrow}$ the electronic state of the system, LS or HS, depends on its history and hence on the information which has been stored. Spin transitions ranging from gradual to abrupt but occurring without hysteresis have been classified as continuous, those occurring with hysteresis as discontinuous.⁷

For several years, we have been interested in synthesizing and exploring the physical properties of

[†] Institut de Chimie de la Matière Condensée de Bordeaux, UPR CNRS no. 9048.

[§] Johannes Gutenberg University.

(1) Sorai, S.; Seki, S. *J. Phys. Chem. Solids* **1974**, *35*, 555.

(2) Goodwin, H. A. *Coord. Chem. Rev.* **1976**, *18*, 293.

(3) Gütlich, P. *Struct. Bonding (Berlin)* **1981**, *44*, 83.

(4) König, E.; Ritter, G.; Kulshreshtha, S. K. *Chem. Rev.* **1985**, *85*, 5, 219.

(5) Beattie J. K. *Adv. Inorg. Chem.* **1988**, *32*, 1.

(6) König, E. *Struct. Bonding (Berlin)* **1991**, *76*, 51.

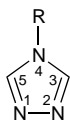
(7) Gütlich P., Hauser, A.; Spiering, H. *Angew. Chem., Int. Ed. Engl.* **1994**, *33*, 2024.

(8) (a) Kahn, O. *Curr. Opin. Sol. State Mater. Sci.* **1996**, *1*, 547. (b) Kahn, O.; Codjovi, E.; Garcia, Y.; van Koningsbruggen, P. J.; Lapouyade, R.; Sommier, L. In *Molecule-Based Magnetic Materials*; Turnbull, M. M., Sugimoto, T., Thompson, L. K., Eds.; Symposium Series No. 644; American Chemical Society: Washington, DC, 1996; p 298.

(9) Kahn, O. *Molecular Magnetism*; VCH: New York, 1993.

(10) Kahn, O.; Jay-Martinez, C. *Science* **1998**, *279*, 44.

strongly cooperative spin transition systems. This led us to focus on spin transition polymeric compounds.^{8b,10–17} The basic idea is that in such compounds the active sites are linked to each other by chemical bridges through which the intersite interaction may be efficiently propagated. Along this line we have extensively investigated the $\text{Fe}^{2+}/4\text{-R-1,2,4-triazole}/\text{A}^-/\text{H}_2\text{O}$ system, where 4-R-1,2,4-triazole, noted hereafter as Rtrz, is the molecule shown below:



and A^- an anion. Most of the compounds have the general formula $[\text{Fe}(\text{Rtrz})_3]\text{A}_2 \cdot n\text{H}_2\text{O}$ where n stands for the number of noncoordinated water molecules. The noncoordinating character of the water molecules may be unambiguously deduced from the occurrence of the spin transition. As a matter of fact, an Fe^{2+} ion with a water molecule in its coordination sphere is HS at any temperature.⁷ So far, no single-crystal suitable for X-ray diffraction could be obtained. However, rather precise structural information has been deduced from EXAFS (X-ray absorption fine structure) at the iron edge¹⁸ and LAXS (large angle X-ray scattering)¹⁹ spectra. For all the compounds investigated so far, the structure most probably consists of linear chains in which the neighboring iron atoms are triply bridged by Rtrz ligands through the nitrogen atoms occupying the 1- and 2-positions. A crystal structure of the same type, with Cu^{2+} replacing Fe^{2+} , was solved. It shows linear chains of triply bridged metal ions.²⁰ Interestingly, this Cu^{2+} compound also contains three noncoordinating water molecules located between the chains. The Fe^{2+} polymeric compounds present a pronounced thermochromism effect accompanying the spin transition. In the LS state they are pink or violet; they absorb around

520 nm (${}^1\text{A}_{1g} \rightarrow {}^1\text{T}_{2g}$). In the HS state they are white; the d–d absorption of lowest energy (${}^5\text{T}_{2g} \rightarrow {}^5\text{E}_g$) occurs in the near-infrared. Several other groups have investigated the same family of compounds.^{21–28}

During the exploration of the $\text{Fe}^{2+}/4\text{-R-1,2,4-triazole}/\text{A}^-/\text{H}_2\text{O}$ system, we discovered an unusual spin transition behavior for the compound of formula $[\text{Fe}(\text{hyetrz})_3](3\text{-nitrophenylsulfonate})_2 \cdot 3\text{H}_2\text{O}$ with hyetrz = 4-(2'-hydroxyethyl)-1,2,4-triazole. This paper is devoted to a detailed investigation of this compound, abbreviated as $\mathbf{1} \cdot 3\text{H}_2\text{O}$. A preliminary report of this work was already published.²⁹

Experimental Section

Syntheses. The ligand hyetrz was synthesized from monoformyl hydrazine, triethylorthoformate, and 2-ethanolamine according to the method described by Bayer et al.³⁰ The iron(II) salt $[\text{Fe}(\text{H}_2\text{O})_6](3\text{-nitrophenylsulfonate})_2$ was obtained as follows: An aqueous solution (60 mL) containing 16.27 g (72.36 mmol) of sodium 3-nitrophenylsulfonate was heated at 80 °C and then added to an aqueous solution (15 mL) containing 7.18 g (36.11 mmol) of iron(II) chloride tetrahydrate and a small amount of ascorbic acid. The volume of the solution was reduced to 20 mL, and the solution was left overnight at room temperature. Large plate-shaped yellow single crystals appeared. They were filtered, washed with water, and dried in a desiccator. Anal. Calcd for $\text{C}_{12}\text{H}_{20}\text{N}_2\text{O}_{16}\text{S}_2\text{Fe}$: C, 25.36; H, 3.55; N, 4.93; S, 11.28; Fe, 9.83. Found: C, 25.42; H, 3.40; N, 4.91; S, 11.50; Fe, 9.83.

$[\text{Fe}(\text{hyetrz})_3](3\text{-nitrophenylsulfonate})_2 \cdot 3\text{H}_2\text{O}$ ($\mathbf{1} \cdot 3\text{H}_2\text{O}$) was synthesized as follows: a methanolic solution (20 mL) containing 3 mmol (1.72 g) of $[\text{Fe}(\text{H}_2\text{O})_6](3\text{-nitrophenylsulfonate})_2$ and a few milligrams of ascorbic acid was heated at 60 °C and added under stirring to a methanolic solution (10 mL) containing 9.1 mmol (1.03 g) of hyetrz. A white precipitate was formed immediately. It was filtered, washed with methanol, and dried in air. During the drying process the compound changes color, from white to pink. Anal. Calcd for $\text{C}_{24}\text{H}_{35}\text{N}_{11}\text{O}_{16}\text{S}_2\text{Fe}$ ($\mathbf{1} \cdot 3\text{H}_2\text{O}$): C, 33.77; H, 4.13; N, 18.05; S, 7.51; Fe, 6.54. Found: C, 33.50; H, 3.99; N, 18.28; S, 6.66; Fe, 6.44.

Physical Measurements. *Optical Detection of the Spin Transition.* This was achieved through the reflectance of the material at 520 nm, using the setup described elsewhere.^{14,15}

Thermogravimetric Measurements. These were carried out with a Setaram apparatus in the 300–400 K temperature range under ambient atmosphere.

Differential Scanning Calorimetry. The DSC experiments were performed with a Perkin-Elmer DSC-7 instrument working down to 100 K. The compounds were sealed in aluminum sample holders. Temperatures and enthalpies were calibrated using the two crystal–crystal transitions of a pure cyclopentane sample (122.0 K, 4871 J mol⁻¹ and 131.8 K, 346.5 J mol⁻¹). The temperatures were determined with a ± 0.1 K accuracy, and the uncertainty of the enthalpy values was estimated as ± 0.1 J mol⁻¹. The experiments in the cooling mode were carried out in a He gas atmosphere, and those in the warming mode under ambient air. The velocities of heating and cooling were fixed at 1 K min⁻¹.

Magnetic Susceptibility Measurements. These were performed under ambient atmosphere with two DSM-8 suscep-

- (11) Kahn, O.; Kröber, J.; Jay, C. *Adv. Mater.* **1992**, *4*, 718.
 (12) Kröber, J.; Codjovi, E.; Kahn, O.; Grolrière, F.; Jay, C. *J. Am. Chem. Soc.* **1993**, *115*, 9810.
 (13) Kröber, J.; Audière, J. P.; Claude, R.; Codjovi, E.; Kahn, O.; Haasnoot, J. G.; Grolrière, F.; Jay, C.; Bousseksou, A.; Linares, J.; Varret, F.; Gonthier-Vassal, A. *Chem. Mater.* **1994**, *6*, 1404.
 (14) Kahn, O.; Codjovi, E. *Philos. Trans. R. Soc. London* **1996**, *A354*, 359.
 (15) Codjovi, E.; Sommier, L.; Kahn, O.; Jay, C. *New J. Chem.* **1996**, *20*, 503.
 (16) van Koningsbruggen, P. J.; Garcia, Y.; Codjovi, E.; Lapouyade, R.; Kahn, O.; Fournès, L.; Rabardel, L. *J. Mater. Chem.* **1997**, *7*, 2069.
 (17) Kahn, O.; Sommier, L.; Codjovi, E. *Chem. Mater.* **1997**, *9*, 3199.
 (18) (a) Michalowicz, A.; Moscovici, J.; Ducourant B.; Cracco, D.; Kahn, O. *Chem. Mater.* **1995**, *7*, 1833. (b) Michalowicz, A.; Moscovici, J.; Kahn, O. *J. Phys. IV* **1997**, *7*, 633. (c) Bausk, N. V.; Erenburg, S. B.; Lavrenova, L. G.; Mazalov, L. N. *J. Struct. Chem.* **1994**, *35*, 509.
 (d) Erenburg, S. B.; Bausk, N. V.; Lavrenova, L. G.; Vamek, V. A.; Mazalov, L. N. *Solid State Ionics* **1997**, *101–103*, 571.
 (19) Verelst, M.; Sommier, L.; Lecante, P.; Mosset, A.; Kahn, O. *Chem. Mater.* **1998**, *10*, 980.
 (20) Garcia, Y.; van Koningsbruggen P. J.; Bravic, G.; Guionneau, P.; Chasseau, D.; Cascarano, G. L.; Moscovici, J.; Lambert, K.; Michalowicz, A.; Kahn, O. *Inorg. Chem.* **1997**, *36*, 6357.
 (21) Haasnoot, P. G. In *Magnetism: a Supramolecular Function*; Kahn, O., Ed.; Kluwer Academic: Dordrecht, The Netherlands, 1996; p 299.
 (22) Lavrenova, L. G.; Ikorskii, V. N.; Varnek, V. A.; Oglezneva, I. M.; Larionov, S. V. *Koord. Khim.* **1986**, *12*, 207; *J. Struct. Chem.* **1993**, *34*, 960.
 (23) Sugiyarto, K. H.; Goodwin, H. A. *Aust. J. Chem.* **1994**, *47*, 263.
 (24) Lavrenova, L. G.; Ikorskii, V. N.; Varnek, V. A.; Oglezneva, I. M.; Larionov, S. V. *Koord. Khim.* **1990**, *16*, 654.

- (25) Lavrenova, L. G.; Yudina, N. G.; Ikorskii, V. N.; Varnek, V. A.; Oglezneva, I. M.; Larionov, S. V. *Polyhedron* **1995**, *14*, 1333.
 (26) Bausk, N. V.; Erenburg, S. B.; Lavrenova, L. G.; Mazalov, L. N. *J. Struct. Chem.* **1995**, *36*, 925.
 (27) (a) Varnek, V. A.; Lavrenova, L. G.; Shipachev, V. A. *J. Struct. Chem.* **1996**, *37*, 165. (b) Varnek, V. A. *J. Struct. Chem.* **1996**, *37*, 514.
 (28) Bronisz, R.; Drabent, K.; Polomka, P.; Rudolf, M. F. *Conference Proceedings, ICAME95*, **1996**, *50*, 11.
 (29) Garcia, Y.; van Koningsbruggen, P. J.; Codjovi, E.; Lapouyade, R.; Kahn, O.; Rabardel, L. *J. Mater. Chem.* **1997**, *7*, 857.
 (30) Bayer, H. O.; Cook, R. S.; von Meyer, W. C. U.S. Patent 3,821,376, 1974.

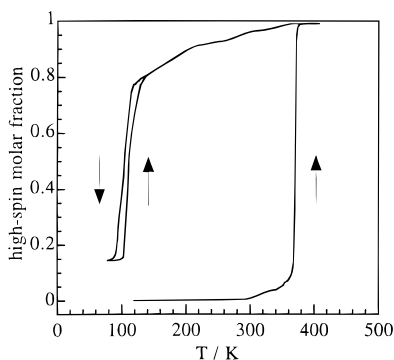


Figure 1. Optical detection of the spin state as a function of temperature for $1 \cdot 3\text{H}_2\text{O}-1$.

tometers, one working in the 77–400 K temperature range, the other one in the 4.2–300 K temperature range. Magnetic data were corrected for magnetization of the sample holder and for diamagnetic contributions, which were estimated from the Pascal constants. Magnetic susceptibilities under pressure were measured in the 20–315 K temperature range using a PAR 151 Foner type magnetometer. The hydrostatic high-pressure cell with silicon oil as a pressure transmitting media had the following characteristics: weight ca. 8 g, pressure range 1–13 kbar, accuracy of pressure determination ca. 0.5 kbar. The sample dimensions were diameter 1 mm, length 5–7 mm. The pressure measurement was achieved using the known pressure dependence of a superconducting transition of an inner tin manometer.

^{57}Fe Mössbauer Measurements. These were performed using a constant acceleration Halder-type spectrometer with a room temperature ^{57}Co source (Rh matrix) in transmission geometry. All reported isomer shifts refer to natural iron at room temperature. The spectra were fitted to a sum of Lorentzians by least-squares refinement.

X-ray Powder Patterns. They were recorded at various temperatures between 70.4 and 358 K, using a Philips PW 1710 counter diffractometer working with $\text{Cu K}\alpha$ radiation. The samples were mounted on the support with silicon grease.

Results of Physical Studies

Optical Detection of the Spin State. The temperature dependence of the spin state of the system was investigated using the optical setup described elsewhere.^{14,15} This setup records the change in reflectivity at 520 nm, characteristic of the LS state. The results are displayed in Figure 1. At room temperature, the material is pink and in the LS state. As the sample is heated monotonically at the rate of 1 K min^{-1} , an exceptionally abrupt transition takes place at 370 K, after which the sample is heated further up to 400 K. As the sample is cooled, the material remains white and in the HS state down to 100 K, where a $\text{HS} \rightarrow \text{LS}$ transition is observed. A second heating experiment from ca. 90 K reveals a $\text{LS} \rightarrow \text{HS}$ transition at about 110 K. This thermal hysteresis of about 10 K is retained over successive thermal cycles. The transition observed at 370 K actually depends on the heating rate. Decreasing this heating rate results in a shift of the transition toward the low temperatures. For instance, the transition is observed at 332 K as the sample is heated at a rate of 0.5 K min^{-1} .

A subsequent experiment was carried out that provides further information on the transition occurring at high temperature. The sample was heated to 320 K and then maintained at that temperature, and the HS molar fraction was followed as a function of time through the

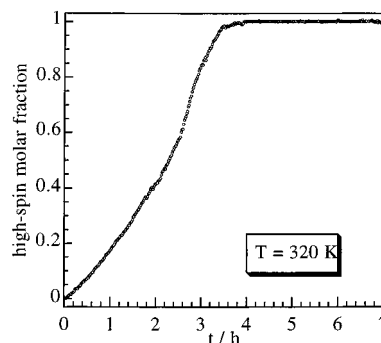


Figure 2. Molar fraction of HS sites at 320 K as a function of time for $1 \cdot 3\text{H}_2\text{O}-1$.

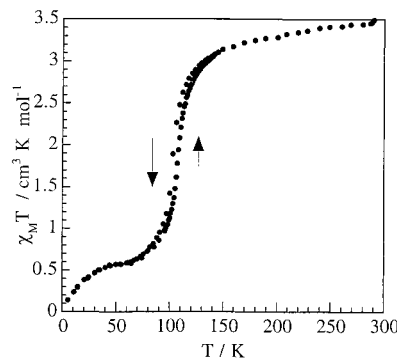


Figure 3. $\chi_M T$ versus T plots both in the cooling and warming modes for compound **1** in the 4.2–300 K temperature range.

normalized reflectivity at 520 nm. The results are shown in Figure 2. The $\text{LS} \rightarrow \text{HS}$ transformation takes place very progressively at 320 K and then is essentially complete after 4 h. This experiment unambiguously indicates that under these experimental conditions the $\text{LS} \rightarrow \text{HS}$ transformation is concomitant with the loss of the three water molecules. The extremely abrupt transition at 370 K observed in Figure 1 is due to a time effect, as already observed in other compounds.³¹ The water release is followed by the reorganization of the lattice, whose rate determines the $\text{LS} \rightarrow \text{HS}$ transition. It is also possible that the rate of the spin transition is determined by the water release process. The metastable LS state transforms abruptly into the stable HS at 370 K under the experimental conditions of Figure 1. This situation appears clearly when comparing this Figure 1 with the thermogravimetry data of Figure 5 (vide infra).

Magnetic Measurements. The temperature dependence of the molar magnetic susceptibility was measured both in the 293–400 K temperature range for $1 \cdot 3\text{H}_2\text{O}-1$ and in the 4.2–293 K temperature range for the dehydrated material **1**, using two different apparatuses. The data above room temperature are in line with the optical data of Figure 1, except that the $\text{LS} \rightarrow \text{HS}$ transition is observed around 350 K instead of 370 K. This difference of temperature is due to the fact that the heating modes are not the same in the two experiments. In the optical study the temperature rose monotonically at the rate of 1 K min^{-1} ; in the magnetic study the susceptibility was measured every 2 K, and in order to reach thermal equilibrium, the temperature

(31) Adler, P.; Spiering, H.; Gülich, P. *J. Phys. Chem. Solids* **1989**, *50*, 587.

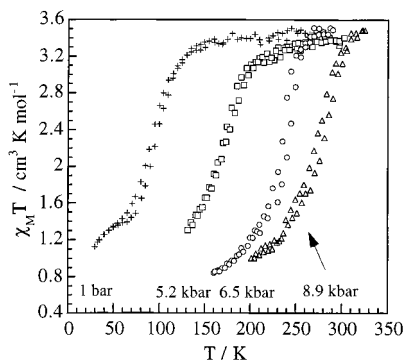


Figure 4. $\chi_M T$ versus T plots for compound **1** in the 20–300 K temperature range, under different pressures up to 8.9 kbar.

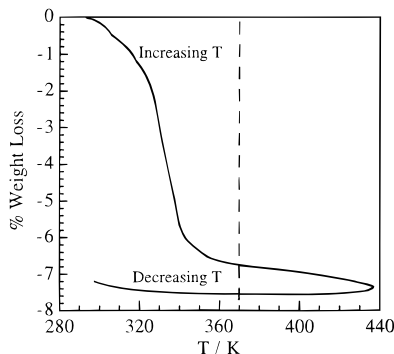


Figure 5. Percentage weight loss versus temperature for **1**· $3\text{H}_2\text{O}$.

oscillated around the fixed value during a few minutes. Remember that the transition is observed optically at 332 K when the heating rate is 0.5 K min^{-1} . Here, we are dealing with a phase transformation in a nonequilibrium state, and the transformation temperature depends dramatically on the experimental conditions. Below room temperature, the magnetic data for **1** are displayed in Figure 3 in the form of the $\chi_M T$ versus T plot, χ_M being the molar magnetic susceptibility and T the temperature. These magnetic data are again in line with the optical data and in the meantime provide more information. At room temperature, $\chi_M T$ is equal to $3.45 \text{ emu K mol}^{-1}$. As T is lowered, $\chi_M T$ decreases very smoothly down to 140 K, reaches $3.05 \text{ emu K mol}^{-1}$ at that temperature, and then decreases very rapidly in the 140–60 K temperature range. Below 60 K, $\chi_M T$ shows a plateau, with a value of $0.55 \text{ emu K mol}^{-1}$, and finally falls down below 50 K. As the temperature is increased, much the same behavior is observed, with a thermal hysteresis of 10 K around 105 K. The $\chi_M T$ value at room temperature exactly corresponds to what is expected for a HS compound. The very smooth decrease of $\chi_M T$ beginning just below room temperature may have two origins, either a very gradual HS \rightarrow LS transformation beginning immediately below 293 K or an intrachain antiferromagnetic interaction between the HS Fe^{2+} ions. In any case, the HS \rightleftharpoons LS transformations are much more abrupt in the 60–140 K temperature range with inversion temperatures found as $T_{1/2}^{\uparrow} = 110 \text{ K}$ and $T_{1/2}^{\downarrow} = 100 \text{ K}$. The HS \rightarrow LS transition is not complete at low temperature. About 15% of the Fe^{2+} ions remain in the HS state around 50 K. The fall of $\chi_M T$ below 50 K is probably due to the zero-field splitting of the HS Fe^{2+} ions and the preferred Boltzmann

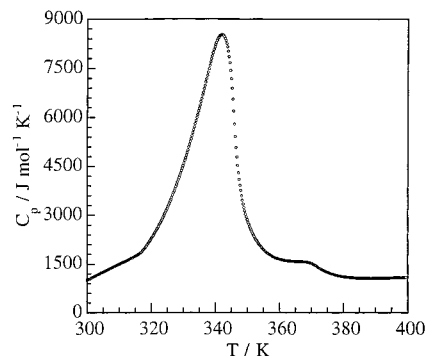


Figure 6. DSC curve for **1**· $3\text{H}_2\text{O}$ above room temperature.

population of the lowest levels with decreasing temperatures.

The magnetic properties of compound **1** were also investigated under pressure up to ca. 9 kbar. The results are shown in Figure 4. Comparing the ambient pressure curve of Figure 4 with Figure 3, one notices that the low-temperature values of $\chi_M T$ are somewhat higher in the former. This is due to the fact that it was not possible to obtain precise $\chi_M T$ values in the pressure experiments. As a matter of fact, these experiments were performed on a very small amount of material, and the sample weight was not accurately known. Furthermore, for technical reasons, the raw data were strongly influenced by the pressure cell. Both error sources by no means perturb the essence of the results. As the pressure increases, a shift toward higher temperatures was observed. However, the profile of the $\chi_M T$ versus T curves remains essentially unchanged, as shown in Figure 4. In particular, the thermal hysteresis width of 10 K was surprisingly retained, whatever the pressure value. The center of the hysteresis loop was observed at 170 K under 5.2 kbar, at 235 K under 6.5 kbar, and at 275 K under 8.9 kbar.

Thermogravimetric and Calorimetric Measurements. The thermogravimetric curve is shown in Figure 5. The velocity of heating was 1 K min^{-1} as for the optical measurements. A continuous loss of mass occurs as T is increased from room temperature and is particularly rapid in the 325–340 K temperature range, after which it continues in a smoother fashion. At 370 K the loss of mass corresponds to three water molecules. As the temperature was lowered, no change in the mass was observed, which indicates that the sample is not rehydrated under the experimental conditions.

The DSC curve above room temperature at the velocity of 1 K min^{-1} is displayed in Figure 6. This curve presents an intense endothermic peak in the 320–355 K temperature range and a much weaker endothermic peak around 370 K. The total enthalpy change was found to be $156.4 \text{ kJ mol}^{-1}$ and the total entropy change to be $400 \text{ J K}^{-1} \text{ mol}^{-1}$. The enthalpy and entropy contributions associated with the small peak of heat capacity around 370 K were estimated as 1.0 kJ mol^{-1} and $2.8 \text{ J K}^{-1} \text{ mol}^{-1}$, respectively. These latter values are much smaller than expected for a LS \rightarrow HS transition. Most of the enthalpy and entropy changes arising from the spin transition occur below 360 K. The $\Delta H = 156.4 \text{ kJ mol}^{-1}$ and $\Delta S = 400 \text{ J K}^{-1} \text{ mol}^{-1}$ values may be attributed to the release of three water molecules together with the LS \rightarrow HS transition. As a

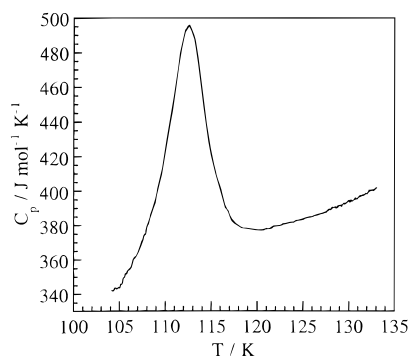


Figure 7. DSC curve for **1** below room temperature.

matter of fact, the total entropy change of ca. $400 \text{ J K}^{-1} \text{ mol}^{-1}$ presumably comprises three contributions arising from (i) release of three water molecules, (ii) LS \rightarrow HS conversion, (iii) structural rearrangement. The entropy change of the dehydration process is estimated to be ca. $100 \text{ J K}^{-1} \text{ mol}^{-1}$. This estimate is based on tabulated standard entropy data of hydrated compounds.³² The entropy change due to the change of spin state originated from a magnetic part, $\Delta S = R \ln[(2S + 1)_{\text{HS}}/(2S + 1)_{\text{LS}}] = 13.4 \text{ J K}^{-1} \text{ mol}^{-1}$, with a major part coming from intra- and intermolecular vibrations amounts to typically $50\text{--}90 \text{ J K}^{-1} \text{ mol}^{-1}$ for mononuclear spin crossover compounds.⁴ For the polymeric compound $[\text{Fe}(\text{Htrz})_2(\text{trz})](\text{BF}_4)$ exhibiting a very cooperative spin transition with $T_{1/2}^{\uparrow} = 383 \text{ K}$ and $T_{1/2}^{\downarrow} = 345 \text{ K}$, however, we have found an entropy change of about $75 \text{ J K}^{-1} \text{ mol}^{-1}$.¹³ Thus, an upper limit of ca. $80 \text{ J K}^{-1} \text{ mol}^{-1}$ as contribution from the spin state conversion appears to be realistic. Finally, there remain ca. $220 \text{ J K}^{-1} \text{ mol}^{-1}$ as major part for the process $\mathbf{1}\cdot\mathbf{3H}_2\mathbf{O}$ (LS) \rightarrow **1** (HS). This part is due to a structural rearrangement, most probably a first-order structural phase change.

The DSC curve for T rising from 100 to 140 K is represented in Figure 7. This curve shows an endothermic peak around 110 K. This peak is obviously related to the spin transition for compound **1** detected from both optical and magnetic studies. It is unfortunately impossible to deduce from this curve the enthalpy and entropy variations associated with this peak, as the heat capacity cannot be measured below 100 K with our equipment.

X-ray Powder Patterns. The X-ray powder patterns of $\mathbf{1}\cdot\mathbf{3H}_2\mathbf{O}$ in the LS state and **1** in the HS state were recorded at room temperature. The former compound is very well crystallized, and the latter is still crystallized, but less well. The recording of a pattern takes about 4 h, so that it was not possible to obtain the pattern of compound **1** in the metastable LS state. The progressive transformation $\mathbf{1}\cdot\mathbf{3H}_2\mathbf{O}$ (LS) \rightarrow **1** (HS) at 320 K detected optically (see Figure 2) was confirmed by X-ray diffraction; Figure 8 displays the X-ray powder pattern at 293 K [$\mathbf{1}\cdot\mathbf{3H}_2\mathbf{O}$ (LS)], at 320 K after 2 h [mixture of $\mathbf{1}\cdot\mathbf{3H}_2\mathbf{O}$ (LS) and **1** (HS)], and after 20 h [pure **1** (HS)]

Mössbauer Spectra. The Mössbauer spectrum of $\mathbf{1}\cdot\mathbf{3H}_2\mathbf{O}$ was recorded at room temperature. This spectrum is characteristic of a LS $\text{Fe}^{\text{II}}\text{N}_6$ site, with however a small amount, ca. 8%, of a HS sites. The temperature

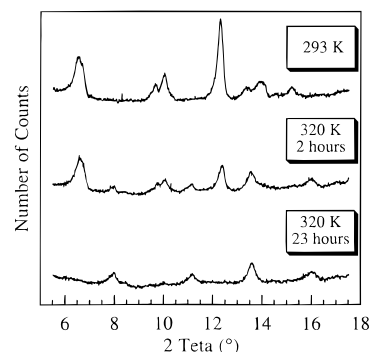


Figure 8. X-ray patterns for $\mathbf{1}\cdot\mathbf{3H}_2\mathbf{O}$ –**1** at 293 K [$\mathbf{1}\cdot\mathbf{3H}_2\mathbf{O}$ (LS)], at 320 K after 2 h [mixture of $\mathbf{1}\cdot\mathbf{3H}_2\mathbf{O}$ (LS) and **1** (HS)], and after 20 h [pure **1** (HS)].

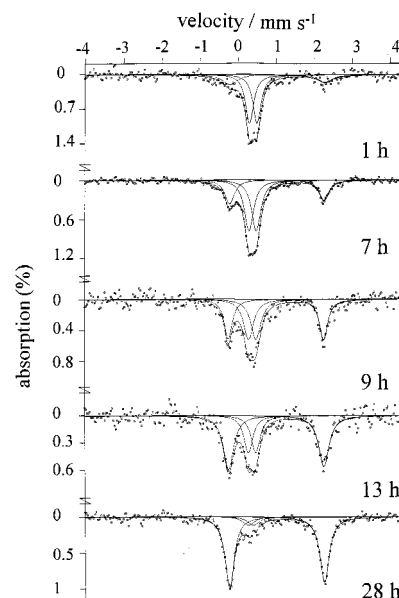


Figure 9. Selected Mössbauer spectra for $\mathbf{1}\cdot\mathbf{3H}_2\mathbf{O}$ –**1** at 320 K as a function of time.

Table 1. Evolution of the Mössbauer Parameters as a Function of Time at 320 K for Compounds $\mathbf{1}\cdot\mathbf{3H}_2\mathbf{O}$ –1**^a**

time (h)	δ (LS) (mm s ⁻¹)	ΔE_Q (LS) (mm s ⁻¹)	δ (HS) (mm s ⁻¹)	ΔE_Q (HS) (mm s ⁻¹)	A_{HS} (%)
1	0.420(6)	0.196(6)	1.05(8)	2.50(8)	26.22
5	0.414(7)	0.188(7)	1.04(2)	2.48(2)	26.39
6	0.410(6)	0.190(6)	1.04(1)	2.48(1)	28.89
7	0.408(6)	0.189(6)	1.04(1)	2.47(1)	31.20
8	0.408(5)	0.189(5)	1.04(1)	2.49(1)	33.75
9	0.40(1)	0.19(1)	1.01(2)	2.50(2)	44.42
13	0.39(2)	0.19(2)	1.02(1)	2.50(1)	61.94
15	0.40(4)	0.17(4)	1.02(1)	2.49(1)	63.92
24	0.37(1)	0.21(1)	1.032(5)	2.490(5)	79.84
28	0.35(8)	0.13(8)	1.032(7)	2.492(7)	85.71

^a δ = isomer shift, ΔE_Q = quadrupole splitting, A_{HS} = area fraction of the HS doublets. Statistical standard deviations are given in parentheses.

of the sample was then warmed to 320 K, and the spectrum was recorded every hour at that temperature. Some selected spectra are displayed in Figure 9, and detailed values of the Mössbauer parameters deduced from least-squares fitting procedures are listed in Table 1. The starting material $\mathbf{1}\cdot\mathbf{3H}_2\mathbf{O}$ in the LS state is progressively transformed into the dehydrated material **1** in the HS state.

The Mössbauer spectra of compound **1** were also studied below room temperature, down to 4.2 K. Some

(32) *Handbook of Chemistry and Physics*, 75th ed.; the Chemical Rubber Compan: Cleveland, Ohio, 1995.

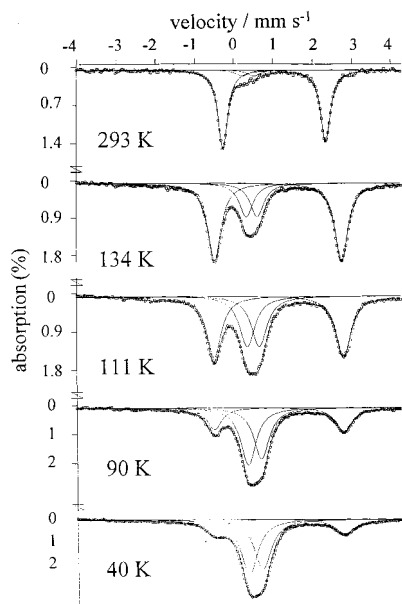


Figure 10. Selected Mössbauer spectra for **1** as a function of temperature below room temperature.

of them are represented in Figure 10, and the values of the Mössbauer parameters are listed in Table 2. At room temperature, the spectrum shows essentially the HS doublet, but a small amount (ca. 8%) of the LS doublet can also be observed. The relative intensity of this LS doublet increases smoothly as the temperature is lowered down to 130 K and then much more rapidly around 100 K. At 40 K, the molar fraction of HS sites is about 20%. The spin transition curve deduced from Mössbauer spectroscopy coincides with the magnetic curve.

Influence of Noncoordinated Solvent Molecules.

The presence of three noncoordinated water molecules plays a crucial role in the stabilization of the LS state. Let us investigate further the influence of these lattice solvent molecules.

The synthesis of $\mathbf{1} \cdot 3\text{H}_2\text{O}$ is carried out in methanol and leads first to a white powder which turns pink when left in the atmosphere, as a result of the uptake of three water molecules. The white compound formulated as $\mathbf{1} \cdot n\text{CH}_3\text{OH}$ can be isolated; it remains white in the presence of methanol vapor. The temperature dependence of $\chi_{\text{M}}T$ was measured both in the cooling and warming mode and revealed rather abrupt spin transitions with $T_{1/2}^{\uparrow} = 180$ K and $T_{1/2}^{\downarrow} = 170$ K. Under vacuum at room temperature the noncoordinated solvent molecules are expelled and another white compound denoted $\mathbf{1}'$ was obtained. X-ray diffraction shows the amorphous character of $\mathbf{1}'$, which displays a very gradual and incomplete spin transformation covering the 100–300 K temperature range, with $T_{1/2}$ around 200 K. From this amorphous powder the abrupt spin transition can be obtained by exposure to water vapor; the crystal lattice of $\mathbf{1} \cdot 3\text{H}_2\text{O}$ is then developed, and the optical and magnetic properties as well as the X-ray pattern described in the preceding section are recovered. If the pink compound $\mathbf{1} \cdot 3\text{H}_2\text{O}$ is now dispersed into methanol, it becomes white and $\mathbf{1} \cdot n\text{CH}_3\text{OH}$ is formed, pointing out the lability of the water molecules which are displaced by the methanol molecules in large excess.

The reaction of $[\text{Fe}(\text{H}_2\text{O})_6](3\text{-nitrophenylsulfonate})_2$ with hyetrz may be carried out in other solvents. For instance, working in dimethylformamide (DMF) affords the compound $\mathbf{1} \cdot \text{DMF}$. The magnetic properties of $\mathbf{1} \cdot \text{DMF}$ are given in Figure 11. Rather abrupt spin transitions are obtained with $T_{1/2}^{\uparrow} = 240$ K and $T_{1/2}^{\downarrow} = 229$ K. Replacing DMF by *N,N*-dimethylacetamide (DMA) affords $\mathbf{1} \cdot \text{DMA}$, whose spin transition loop is shifted toward lower temperatures with $T_{1/2}^{\uparrow} = 155$ K and $T_{1/2}^{\downarrow} = 140$ K. The white compounds $\mathbf{1} \cdot \text{DMF}$ and $\mathbf{1} \cdot \text{DMA}$ also turn pink when left in the proximity of a water source. The water uptake is however much slower than for $\mathbf{1} \cdot n\text{CH}_3\text{OH}$. This role of the solvent molecules is schematized in Figure 12.

Discussion

It has been demonstrated that the title compound may exist in two forms, one with three noncoordinated water molecules ($\mathbf{1} \cdot 3\text{H}_2\text{O}$), the other one without lattice water molecule ($\mathbf{1}$). The hydrated form can be gradually converted into the nonhydrated one by heating the material slowly to ca. 370 K. Both forms differ significantly in their spin transition regime. Compound $\mathbf{1} \cdot 3\text{H}_2\text{O}$ shows LS behavior at room temperature. On heating $\mathbf{1} \cdot 3\text{H}_2\text{O}$ above room temperature, the diamagnetic material loses lattice water and thereby turns to the paramagnetic HS phase. Thus the observed spin transition occurring above room temperature is driven by the release of three noncoordinated water molecules upon heating $\mathbf{1} \cdot 3\text{H}_2\text{O}$. The rate of the spin transition is determined either by the rate of dehydration or by the lattice reorganization following the release of water. The influence of noncoordinated lattice solvent molecules on the spin transition behavior of mononuclear species has been investigated by one of us^{7,35,36} as well as by Goodwin and co-workers.^{38,40} Two factors have been found to be operative, namely hydrogen-bond formation and crystal-packing effects. In the present case the kinetic factors play also a crucial role in the high-temperature transition.

In contrast to other $[\text{Fe}(\text{Rtrz})_3]\text{A}_2 \cdot n\text{H}_2\text{O}$ compounds, $\mathbf{1}$ does not easily reabsorb water at room temperature. In a normal atmosphere, $\mathbf{1}$ is stable for months. On the other hand, if the material is maintained in a closed box in the presence of water, the rehydration happens within 1 h or so, and $\mathbf{1} \cdot 3\text{H}_2\text{O}$ is found again with the same physical properties as the starting material.

The spin transition for $\mathbf{1}$ is rather abrupt with a thermal hysteresis of about 10 K around $T_{1/2} = 100$ K,

(33) (a) Vos, G.; Le Fèvre, R. A.; de Graaff, R. A. G.; Haasnoot, J. G.; Reedijk, J. *J. Am. Chem. Soc.* **1983**, *105*, 1682. (b) Vos, G.; de Graff, R. A. G.; Haasnoot, J. G.; van der Kraan, A. M.; de Vaal, P.; Reedijk, J. *Inorg. Chem.* **1984**, *23*, 2905. (c) Kolnaar, J. J. A.; van Dijk, G.; Kooijman, H.; Spek, A. L.; Ksenofontov, V. G.; Gütllich, P.; Haasnoot, J. G.; Reedijk, J. *Inorg. Chem.* **1997**, *36*, 2433.

(34) Thomann, M.; Kahn, O.; Guilhem, J.; Varret, F. *Inorg. Chem.* **1994**, *33*, 6029.

(35) Köhler, C. P.; Jakobi, R.; Meissner, E.; Wiehl, L.; Spiering, H. Gütllich, P. *J. Phys. Chem. Solids* **1990**, *51*, 239.

(36) Sorai, M.; Enslin, J.; Hasselbach, K. M.; Gütllich, P. *Chem. Phys.* **1977**, *20*, 197.

(37) Gütllich, P.; Köppen, H.; Steinhäuser, H. G. *Chem. Phys. Lett.* **1980**, *74*, 475.

(38) Sugiyarto, H.; Goodwin, H. A. *Aust. J. Chem.* **1988**, *41*, 1645.

(39) Sugiyarto, H.; Graig, D. C.; Rae, A. D.; Goodwin, H. A. *Aust. J. Chem.* **1993**, *46*, 1269.

(40) Sugiyarto, H.; Graig, D. C.; Rae, A. D.; Goodwin, H. A. *Aust. J. Chem.* **1994**, *47*, 869.

these interactions on $T_{1/2}$.^{38–41} Most often water is hydrogen bonded to the ligand through a $\text{N}-\text{H}\cdots\text{OH}_2$ interaction, which results in an increase of the electron density at the nitrogen atom. The metal–ligand interaction is then strengthened, and the LS state is favored. Therefore, $T_{1/2}$ is shifted toward higher temperatures. Sometimes, the main water–ligand interaction occurs through the nitrogen atom of an imine group, $=\text{N}\cdots\text{OH}_2$, which results in a decrease of the electron density on the ligand. The metal–ligand interaction is then weakened, and the HS state is favored; $T_{1/2}$ is shifted downward. Compound $\mathbf{1} \cdot 3\text{H}_2\text{O}$ possesses neither secondary amine nor free imine groups, and the effect of the lattice solvent cannot be attributed to an electronic effect of the ligand induced by the kind of hydrogen bondings discussed above. Disorder–order transitions of the solvent molecules have also been suggested to trigger the spin transition of $[\text{Fe}(\text{2-pic})_3]\text{Cl}_2 \cdot 3\text{H}_2\text{O}$.⁴² In the present case, this mechanism cannot be disregarded. However, the most striking results are the following: (i) A crystalline material exhibiting an abrupt spin transition can be formed through the incorporation of water molecules into an amorphous solid. A similar crystalline structure formation through incorporation of water has recently been observed with a push–pull quinonoid system which in the meantime loses its capability of second-harmonic generation.⁴³ (ii) The thermally dehydrated material $\mathbf{1}$ does not reabsorb water in a normal atmosphere. It may appear surprising that methanol and water can be easily exchanged, for instance during the synthesis of $\mathbf{1} \cdot 3\text{H}_2\text{O}$ from $\mathbf{1} \cdot n\text{CH}_3\text{OH}$. Perhaps, the structure of $\mathbf{1} \cdot \text{S}$ (S stands for solvent molecules) is sufficiently open to allow the exchange of solvent molecules while that of $\mathbf{1}$ is more shrunked and, as in zeolites, its pore size controls the rate of solvent uptake.

Conclusion

The synergy between loss of noncoordinated water molecules and LS \rightarrow HS transition has already been

(41) Sugiyarto, H.; Weitzner, K.; Graig, D. C.; Goodwin, H. A. *Aust. J. Chem.* **1997**, *50*, 869.

(42) Mikami, M.; Konno, M.; Saito, Y. *Chem. Phys. Lett.* **1979**, *63*, 566.

(43) Ravi, M.; Narayana, R.; Cohen, S.; Agranat, I.; Radhakrishnan, T. P. *J. Mater. Chem.* **1996**, *6*, 1853.

observed in other compounds, mononuclear as well as polymeric, but usually the dehydrated HS species is hygroscopic and spontaneously transforms back into the hydrated LS species.¹⁶ In the present case it is not so in a normal atmosphere. Moreover, the spin transition regimes for the hydrated and dehydrated materials are very different, one taking place above room temperature, the other one close to liquid nitrogen temperature. Such a situation suggests some possible applications of the material.¹⁰ For instance, it can be used as a single use display. Such a material can indicate the first utilization of a prepaid stored value card. It can also be used as a temperature threshold indicator. The pink \rightarrow white change of color accompanying the high-temperature transition is irreversible, provided that the user has no access to a liquid nitrogen source. What is promising in terms of applications is that $[\text{Fe}(\text{hyetrz})_3]-(3\text{-nitrophenylsulfonate})_2 \cdot 3\text{H}_2\text{O}$ is not a unique compound. It belongs to a family of compounds behaving in the same way, but whose irreversible and thermochromic LS \rightarrow HS transition covers a temperature range between 20 °C and 100 °C.

We would like to emphasize the richness of properties for this class of $\text{Fe}^{2+}/4\text{-R-1,2,4-triazole}$ spin transition polymers. So far, four different behaviors have been observed, namely, (i) very abrupt transitions with a well-shaped thermal hysteresis (A typical example of such a behavior is offered by $[\text{Fe}(\text{NH}_2\text{trz})_3](\text{NO}_3)_2$.^{8,22}), (ii) smoother spin transitions, occurring over at least 10 K, with a hysteresis width in the range 5–10 K ($[\text{Fe}(\text{NH}_2\text{trz})_3](\text{BF}_4)_2 \cdot \text{H}_2\text{O}$ behaves this way.^{11,24}), (iii) synergy between spin transition and dehydration–rehydration process (That happens, for instance, for $[\text{Fe}(\text{NH}_2\text{trz})_3](\text{tosylate})_2 \cdot 2\text{H}_2\text{O} - [\text{Fe}(\text{NH}_2\text{trz})_3](\text{tosylate})_2$; the dehydrated material is hygroscopic and spontaneously reverts to the hydrated compound.¹⁵), and (iv) finally, the behavior described in this paper. The compounds of this type resemble those described in iii, with however two important differences: the transitions for the dehydrated material occur at much lower temperature than for the hydrated one, and the dehydrated material is stable; under normal conditions it does not reabsorb water.

CM980107+